ANALYSIS OF ELECTRON DENSITY CALCULATIONS USING DETERMINISTIC-PROBABILISTIC MODEL OF THE IONOSPHERIC D-REGION

S.Z. Bekker

Institute of Geosphere Dynamics RAS,
Moscow, Russia, susanna.bekker@gmail.com

Abstract. The work is devoted to the development of a fundamentally new way of modeling the ionospheric D-region – deterministic-probabilistic. The results of N_e calculations using this technique are analyzed. Research of this kind is of fundamental importance, related to the rejection of a purely deterministic description of a continuously changing environment such as the ionosphere. In this work, the electron density is calculated using a five-component system of ionization-recombination cycle equations. Probability density functions (PDFs) of input parameters of the model are used to solve the system. The most important sources of the D-region ionization are taken into account to calculate PDFs of the ionization rate. The necessary number of iterations is determined by the convergence of PDFs of the electron density from 50 km to 85 km at midlatitudes under different heliogeophysical conditions.

Theoretical N_e PDFs have been shown to be in good agreement with two experimental databases on electron density, especially at large D-region heights. The next important stage of modeling is the thorough verification of N_e PDFs from experimental radiophysical data on VLF–LF propagation.

Keywords: modeling of the ionospheric D-region, probabilistic statistical modeling, theory of probability, ionization rate, electron density, VLF–LF propagation.

INTRODUCTION

There is no doubt that the ionosphere as a radio propagation environment significantly affects the operation of radio systems; therefore, compensating for errors in the calculation of radio propagation requires knowing ionospheric parameters in a quite wide range of altitudes and latitudes [Powerful ..., 2013].

Today's commonly used deterministic methods of describing environment ignore irregularity and continuous variability of the ionosphere, and hence are inadequate for real-time correction of radar data. In the last few years, using the ionospheric D-region and VLF–LF propagation through the ionosphere as an example, a principally new direction in modeling – probabilistic-statistical – has been actively developed [Kozlov et al., 2014]. Probabilistic-statistical models provide distribution densities of ionospheric parameters in all combinations of heliogeophysical conditions. These parameters are selected according to their distribution laws and are used for calculating radiophysical values. Ultimately we have wave amplitude and phase PDFs along a selected path and frequency under different solar and magnetic activity conditions, in different latitudes, seasons, and times of day. PDFs of all the above values provide a detailed insight into geophysical and radiophysical conditions along a path, contain information about reliability of communication under particular conditions, and give information about the most and least favorable data transmission conditions to developers of VLF–LF radio systems. This information cannot be derived from deterministic models, regardless of the principles they are built on, how often they are corrected, and how much experimental data they use.

Two directions of the probabilistic-statistical modeling have been validated so far: deterministic-probabilistic and empirical-statistical [Kozlov et al., 2014]. The purpose of this work is to calculate PDFs of N_e, using the deterministic-probabilistic (D-P) approach and analyzing results. This approach relies on theoretical studies (ionization-recombination cycle equations) with varying unknown parameters.

The deterministic-probabilistic modeling consists of the following stages.

1. Determining unknown and most variable parameters of the neutral atmosphere included in equations of the ionization-recombination cycle of the ionospheric D-region.

2. Finding the laws of distribution of these parameters by height under different heliogeophysical conditions from long-term experimental satellite data.

3. Generating N profiles of these parameters according to the obtained distribution functions, using a generator of random numbers (generated values should be described by the same distributions as input experimental data). The number N is determined by convergence of solutions of the ionization-recombination cycle equations.

4. Solving the system of differential equations for each set of generated profiles.

5. Using the resulting N_e profiles as a radio wave propagation medium. Obtaining PDFs of radiophysical parameters along specific VLF paths. Wave amplitude and PDFs are verified using experimental data obtained independently from complex radiophysical studies carried out at the Geophysical Observatory of IDG RAS "Mikhnevo".

IONIZATION-RECOMBINATION CYCLE AND INPUT PARAMETERS OF THE MODEL

To calculate vertical profiles of N_e, the five-component system of differential equations of ioniza-

tion-recombination cycle of the ionospheric D-region, first presented by Egoshin et al. [2012], is used. This system accounts for the main aerodynamic processes affecting the electron density in the lower ionosphere: ionization by solar radiation and cosmic rays q, photo-detachment of electrons from O_2^-, reaction of transformation of NO^+ and O_2^- into positive and negative cluster ions, electron attachment in triple collisions to O_2, dissociative recombination of electrons with positive ions, and ion-ion recombination. This system of equations is stationary and is solved using the relaxation method. The efficiency of the five-component model has been repeatedly tested from geophysical and radio-physical experimental data under quiet conditions and also during solar flares of different classes. At present there are global numerical ionospheric models, e.g. [Krivolutsky et al., 2015], describing the most complete interaction of neutral and charged components at D-region heights and involving hundreds of photochemical reactions. Of course, such models have a higher accuracy than the five-component model; however, to treat the basic principles of the probabilistic modeling of the undisturbed mid-latitude D-region it is more than sufficient to examine the behavior of the main set of charged ionospheric components.

Unknown varying parameters of the system are the ionization rate q, neutral temperature T, concentrations of $[O_2]$, $[N_2]$, $[H_2O]$, $[O_3]$, and $[CO_2]$. A large body of experimental satellite data has been amassed so far on density and temperature of the neutral atmosphere as well as on concentrations of minor neutral components in a wide range of heights and geomagnetic latitudes. Experimental AURA databases on T, $[O_2]$, $[N_2]$, $[H_2O]$, $[O_3]$ and TIMED databases on $[CO_2]$ for 2009, 2010, and 2012 are statistically processed. Four seasons are analyzed: winter (November–February), spring (March, April), summer (May–August), autumn (September, October); the daytime and nighttime are hours of the dayside and nightside ionosphere respectively. The model was built independently under different heliogeophysical conditions, with no consideration given to the diurnal variation in the parameters and to the passage of the terminator because the ionosphere is very unstable during this time. PDFs of T, $[O_2]$, $[N_2]$, $[H_2O]$, $[O_3]$, and $[CO_2]$ are plotted for all combinations of heliogeophysical conditions at $h= 50–85$ km with an increment of 5 km. From the distributions, profiles of the input parameters are generated which are used for solving the system of differential cycle equations. In Figures 1, 2 are PDFs of T and $[N_2]$ at different heights. These data represent the daytime and the autumn equinox period in 2009 (minimum solar activity).
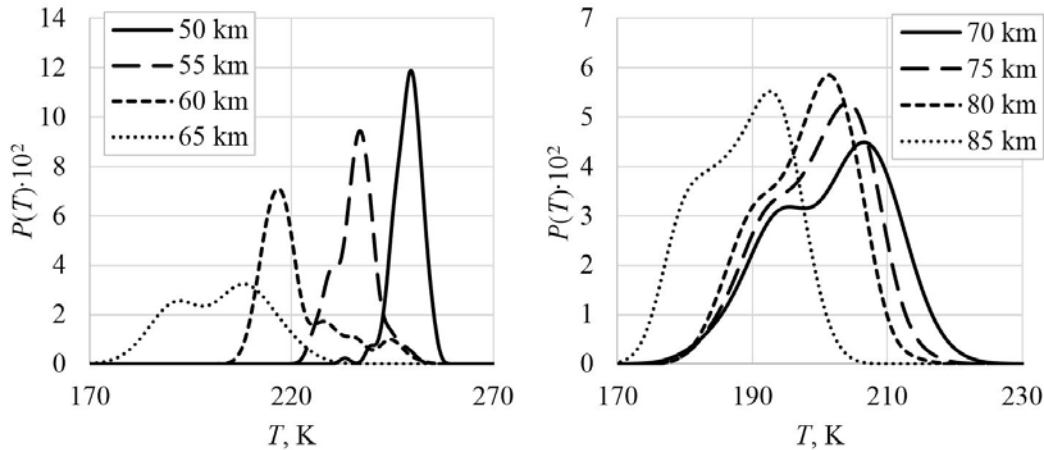

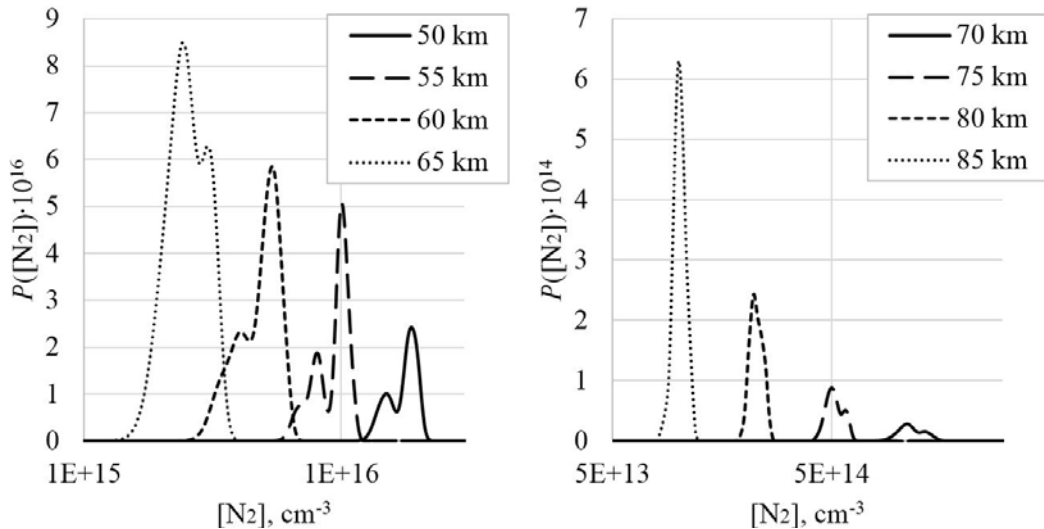*Figure 1.* PDFs of T for $h= 50–85$ km (daytime, autumn equinox period in 2009, midlatitudes)

Figure 2. PDFs of $[N_2]$ for h=50–85 km (daytime, autumn equinox period in 2009, midlatitudes)

It can be seen that it is difficult to describe the curves by any specific distribution laws; therefore it has been decided not to use them but to generate profiles directly according to the empirically derived curves. The number of generated profiles required for convergence of output solutions of the system is discussed below.

The presence of a large amount of satellite data on density and temperature of the lower ionosphere, as well as on concentrations of minor neutral components, allows us to reliably estimate values of all but one of the variable input parameters of the model. The most important and still unresolved problem of modeling is the lack of reliable information about the behavior of one of the most significant parameters of the ionization-recombination cycle – the ionization rate. The analysis of the sensitivity of the solutions of the cycle equations shows that at heights of VLF reflection the behavior of N_e entirely depends just on the q and T variations, which is also natural for purely physical reasons.

IONIZATION RATE CALCULATION

To assess q, the main sources of ionization at heights of the ionospheric D-region are examined.

1. Cosmic-ray ionization

Cosmic rays are the only source of ionization of the lower part of the D-region at $h \approx 50$–65 km. The cosmic ray flux is very small, and hence ionization requires a high concentration of neutrals [M], which is known to decrease with height; therefore above 65 km the cosmic-ray contribution to ionization is insignificant.

The cosmic-ray ionization rate q_{cr} in the lower ionosphere depending on height, latitude, and solar activity can be estimated from parameterized equations derived by Heaps [1978] and presented in Table.

In this work, to verify the results from radiophysical data, the ionization rate is calculated for a particular mid-latitude VLF path.

The DHO transmitter operating at 23.4 kHz is located in Germany (53° N, 8° E), and the receiver is at GPO "Mikhnevo" (56° N, 38° E). Therefore, $\varphi = 54.5°$ is taken and the respective formulas from Table are used.

2. NO ionization by the L_α line ($\lambda = 121.6$ nm)

The question about ionospheric ionization at $h \approx 65$–85 km has always presented the greatest difficulty. The fact is that the radiation with $\lambda < 100$ nm does not penetrate into the D-region heights, and quanta with wavelengths greater than 100 nm have insufficient energy to ionize O_2 and N_2, which constitute the medium at these heights. In this height range there is, however, a minor neutral component that is affected by a softer radiation – nitrogen oxide NO (~9.27 eV ionization potential).

The photoionization rate of the nth component of the neutral gas can be estimated by the formula [Brunelli, Namgaladze, 1988]

$$q_n(h) = n_n(h) j_n(h) =$$
$$= n_n(h) \sigma_{n,\lambda}^{ion} F_\lambda^\infty \exp\left(-\sec\chi \sum_i \sigma_i^{absorp} \int_h^{+\infty} n_i(h)\,dh\right), \quad (1)$$

where n_n is the concentration of the nth component, j_n is the photoionization coefficient, $\sigma_{n,\lambda}^{ion}$ is the cross-section of the nth component photoionization by radiation with

a wavelength λ, F_λ^∞ is the photon flux at a wavelength λ outside the atmosphere, χ is the solar zenith angle, σ_i^{absorp} is the photon-absorption cross-section with a wavelength λ, $\int_h^{+\infty} n_i(h)\,dh$ is the number of molecules of the absorbing component in the column of unit cross-section (cm^{-2}) over a given height h.

Note that Formula (1) is valid only for $\chi < 80°$, and at large zenith angles $\sec\chi$ should be replaced by the Chapman function.

To estimate the NO ionization by the Lyman-alpha (Lα) line in the daytime, we get

$$q_{L\alpha}(h) =$$
$$= \sigma_{NO}^{ion}[NO](h) F_{L\alpha} \exp\left(-\sigma_{O_2}^{absorp} \sec\chi \int_h^{+\infty} [O_2](h)\,dh\right). \quad (2)$$

The mean radiation flux in the daytime is $F_{L\alpha} = 3.49 \cdot 10^{11}\, cm^{-2} s^{-1}$ as derived from measurements made in 2009 [Kotov, 2011]. The O_2 absorption cross-section and NO ionization cross-section required for the calculation are $\sigma_{O_2}^{absorp} = 1.13 \cdot 10^{-20}\, cm^{-2}$ and $\sigma_{NO}^{ion} = 1.86 \cdot 10^{-18}\, cm^{-2}$. The solar zenith angle is given by the expression

$$\cos\chi = \sin\varphi \sin\delta - \cos\varphi \cos\delta \cos(\omega t), \quad (3)$$

where φ is the geographic latitude, t is the time of day, ω is the Earth angular velocity, δ is the solar declination determined as follows:

$$\text{tg}\delta = \text{tg}23.5° \sin\left(\frac{2\pi}{365}(d-80)\right), \quad (4)$$

where d is the day number in the year.

Determination of the [NO] concentration is the most difficult and important step in calculating the ionization rate. It is known that there is a method of estimating the concentration of atmospheric component from its optical emission. Shefov et al. [2006] have studied the NO emission at a wavelength of 5.3 µm and have shown that $Q_{5.3} = k[NO]$, where $Q_{5.3}$ is the NO emission measure at 5.3 µm, k is the proportionality factor, which is a complex function of concentrations of neutral, charged, excited ionospheric components and reaction rate constants, some of which are simply unknown. Nevertheless, the observed proportionality suggests that the behavior of the [NO] PDFs will be absolutely identical to the behavior of PDFs of $Q_{5.3}$, which from the beginning of 2002 is measured with the SABER radiometer, installed in TIMED [http: //saber.gats-inc.com/browse_data.php]. Thus, under different heliogeophysical conditions it remains to determine the reference mean [NO] profiles.

In 1960–70s, a series of rocket experiments was carried out to measure [NO] [Danilov, Ledomskaya, 1984]; however, the use of a single experimental profile is at least incorrect. It is also impossible to average the obtained values because there were a little more than ten experiments, and, of course, it is difficult to extend them to other heliogeophysical conditions.

As reference values for calculating the [NO] concentration we can take USA Standard profiles [Anderson

Cosmic-ray ionization rate for different latitudes φ and solar activity levels

	High solar activity	Low solar activity
$|\varphi|<53°$	$q_{\mathrm{CR}} = \left(1.74\cdot10^{-18} + 1.93\cdot10^{-17}\,|\sin\varphi|^4\right)[\mathrm{M}]$	$q_{\mathrm{CR}} = \left(1.74\cdot10^{-18} + 2.84\cdot10^{-17}\,|\sin\varphi|^4\right)[\mathrm{M}]$
$|\varphi|>53°$	$q_{\mathrm{CR}} = 1.44\cdot10^{-17}\,[\mathrm{M}]$	$q_{\mathrm{CR}} = \left(1.44\cdot10^{-17} + 4.92\cdot10^{-18}\right)[\mathrm{M}]$

et al.,1986], which are given in ppmv (volume concentration in parts per million), and therefore the O_2 and N_2 concentrations from AURA can be used to calculate the profiles for any heliogeophysical conditions in the period of interest. Alternatively, in a range of midlatitudes for heights lower than 90 km we can use the Abby Normal approximation proposed by Schumer [2009] and defined by the expression

$$[\mathrm{NO}] = [\mathrm{O}]/(2\cdot10^4) + [\mathrm{O_2}]/(2\cdot10^7), \tag{5}$$

which puts no restrictions on concentration calculations for different conditions either. The [NO] vertical profiles corresponding to the daytime of the autumn equinox period in 2009 and to the mid-latitude path DHO–Mikhnevo (the region considered is 53°–56° N, 8°–38° E) are compared in Figure 3, *a*. It can be seen that the profiles begin to differ only at $h>75$ km, with the same orders of magnitude throughout the height range under study. Next, the N_e calculation results are given for the two presented curves.

During the nighttime, the source of photoionization is the solar radiation scattered to the night side. Thomas, Bowman [1985] have proposed a night flux approximation at which the last two multipliers of Formula (2) are replaced by a zenith angle and height function, thereby the ionization rate formula takes the form

$$q_{\mathrm{L\alpha}}^{\mathrm{night}}(h) = \sigma_{\mathrm{NO}}^{\mathrm{ion}}[\mathrm{NO}](h)\frac{4.9\cdot10^8}{\cos^2\chi + 0.1}\times$$
$$\times\exp(-0.48\exp(0.15(85-h)-1)). \tag{6}$$

3. $O_2(^1\Delta_g)$ ionization within λ=102.7–111.8 nm

The radiation in the wavelength range between 102.7 and 111.8 nm penetrates into the D-region heights, but the energy of these photons is insufficient to ionize O_2 and N_2. The difference between the quantum energy and the O_2 ionization threshold is less than 1 eV, therefore the energy stored by the excited $O_2(^1\Delta_g)$ molecule is sufficient to compensate for this difference.

Paulsen et al. [1971] have proposed to approximate the $O_2(^1\Delta_g)$ ionization rate in the UV range by the analytical expression

$$q_{\mathrm{UV}}(h) = \left[O_2\left(^1\Delta_g\right)\right]\times$$
$$\times\left(0.549\cdot10^{-9}\exp\left(-2.406\cdot10^{-20}\int_h^{+\infty}[O_2](h)\,dh\right)+\right.$$
$$\left.+2.614\cdot10^{-9}\exp\left(-8.508\cdot10^{-20}\int_h^{+\infty}[O_2](h)\,dh\right)\right). \tag{7}$$

The recommended averaged experimental profile of $O_2(^1\Delta_g)$ is shown in Figure 3, *b*.

4. Energetic particle flux ionization

The nightside mid-latitude D-region is very poorly studied. First of all, this is due to the difficulty in measuring concentrations of its minor components. During the daytime under quiet conditions, the ionization rates which are provided by protons and electrons precipitating from radiation belts are essentially lower than those provided by the NO ionization in the Lα line. However, it has already become clear that precipitating electrons with energies of a few tens of kiloelectronvolts contribute significantly to the ionization of the nightside D-region even at midlatitudes. To account for the rate of ion formation due to the influence of energetic electrons, estimates made by Koshelev [1983] are used.

Ionization by precipitating protons and electrons can be a significant source of daytime ionization of the mid-latitude ionosphere, but only during strong geomagnetic disturbances and solar proton events [Krivolutsky, Repnev, 2009; Krivolutsky et al., 2017].

5. Cumulative ionization

The mean cumulative ionization obtained by accounting for the above daytime and nighttime ionization sources is shown in Figure 4. The calculations have been made for the mid-latitude path DHO–Mikhnevo, using the [NO] profile proposed by Anderson et al. [1986].

It can be seen that the cosmic-ray ionization at high latitudes is virtually independent of the time of day. During the daytime, already at 65 km, the NO ionization in the Lα line becomes significant, the $O_2(^1\Delta_g)$ ionization in the UV range appears even higher, and approximately at 85 km the latter begins to predominate over the NO ionization, but then drops sharply; yet the total ionization of the E-region continues to rise due to the O_2 ionization in the Lβ line. At night, approximately from 65 km, the D-region is ionized by high-energy electrons precipitating from radiation belts. The nighttime ionization of NO are almost imperceptible there.

Figure 5 shows the seasonal dependence of the total ionization rate. Throughout the height range, $\bar{q}$ is greater in summer months, and during the autumn and spring equinoxes the values almost coincide (summer values are by ~20 % more). In winter months above 60 km, ionization is much lower both in the daytime and in the nighttime, and $q_{\mathrm{L\alpha}}$ makes the main contribution to this difference.

The distributions of the [NO] and [M] concentrations throughout the height range allow us to obtain PDFs of the total ionization rate under different heliogeophysical conditions. As an example, Figure 6 shows the q probability density in the daytime of the autumn equinox period in 2009. These distributions as well as the distributions of other input parameters of the model are used for generating vertical profiles, which are substituted in the system of differential ionization-recombination cycle equations.
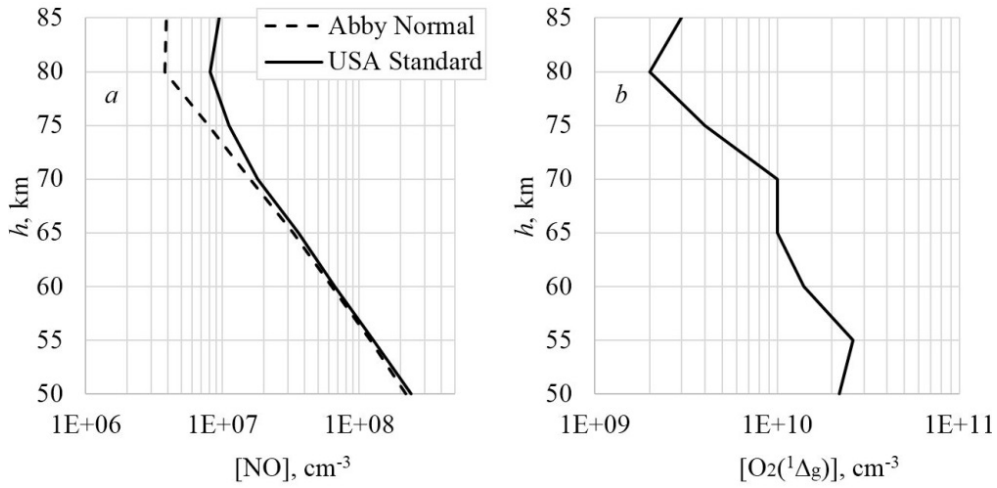
Figure 3. Mean vertical profiles of [NO] (a) and [$O_2(^1\Delta_g)$] profile (*b*) (daytime, autumn equinox period in 2009, midlatitudes)
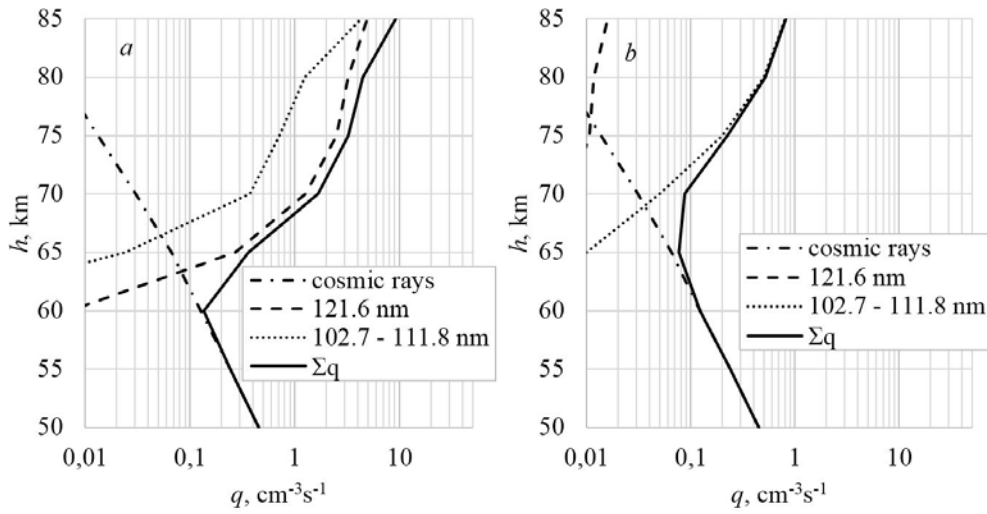

Figure 4. Mean rates of the ionization by different sources in the daytime (*a*) and nighttime (*b*) (autumn equinox period in 2009, midlatitudes)
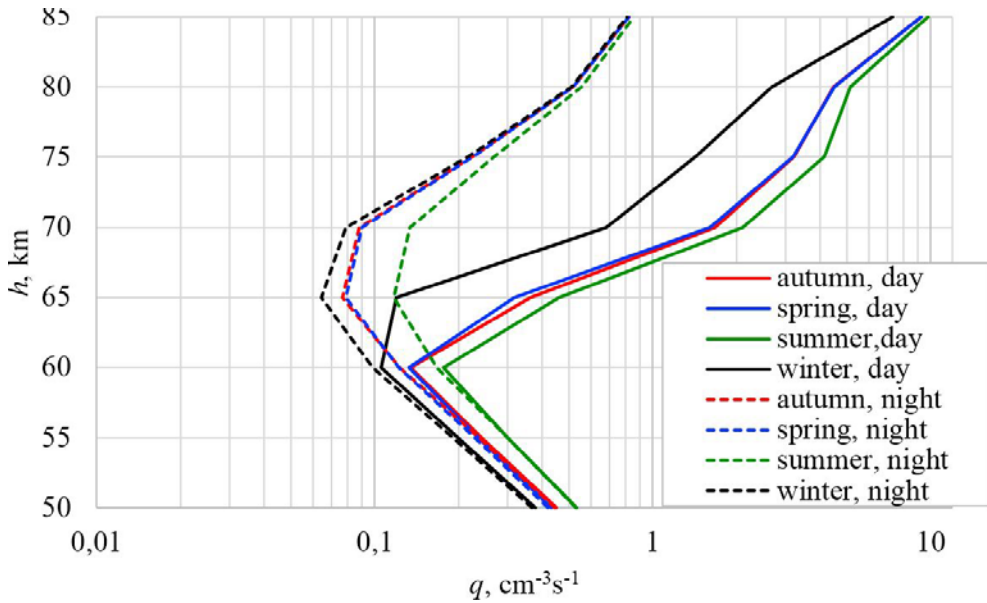

Figure 5. Mean cumulative ionization rates in different seasons and times of day (2009, midlatitudes)
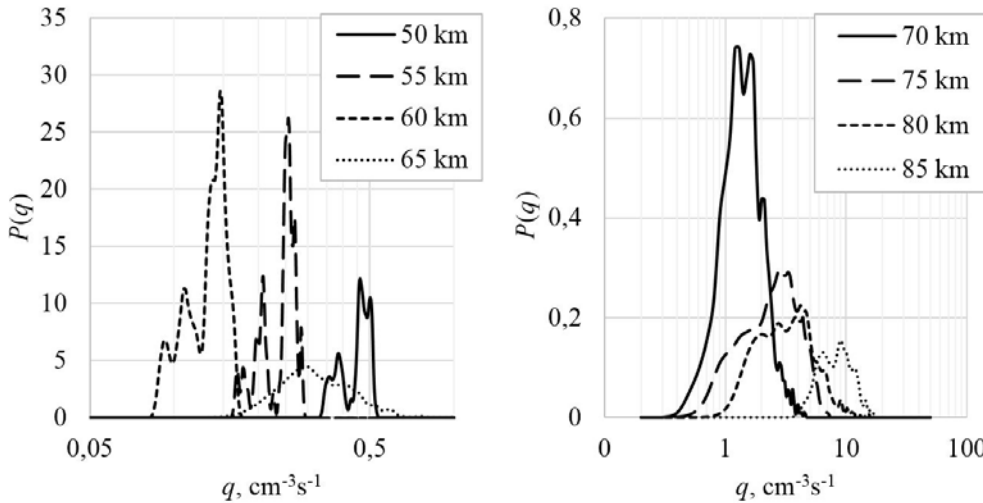
Figure 6. PDFs of q for h= 50–85 km (daytime, autumn equinox period in 2009, midlatitudes)

RESULTS OF ELECTRON DENSITY CALCULATIONS

As discussed above, N_e is calculated using the five-component system of differential equations including N_e, $[NO]$, $[O_2^-]$, $[XY]$, $[XY^-]$ as output parameters, where $[XY]$ and $[XY^-]$ are concentrations of positive and negative cluster ions.

In an increment of 5 km according to the obtained PDFs, N sets of input profiles are generated. Each of these sets is used to solve a system of equations, and at the output N profiles of N_e are obtained. An important part of this task is to determine the number of iterations sufficient for convergence of the probability density N_e under any heliogeophysical conditions of interest. Figure 7 shows PDFs of N_e versus the number of iterations at two heights. The distributions at h=60 km are discretized with an increment of 0.1 cm^{-3}; and at h=80 km, with an increment of 8 cm^{-3}. To assess the convergence, it has been decided to compare the distributions with a conventionally limit curve constructed for N=10000. It turned out that from N=1000 deviations of the distributions from the limit curve do not exceed 2 %. It has been decided that this value is sufficient for convergence of the solution and correct construction of the distributions.

To verify the obtained values of N_e, GOST (All-Union State Standard) R 25645.15-94 of electron density is used. GOST is based on the global model of N_e and effective electron-collision frequency in the lower ionosphere, constructed from the results of matching between calculated and experimental data on predominantly VLF radio wave propagation. Figure 8, *a* depicts theoretically obtained $\overline{N}_e$ for two different [NO] profiles (Abby Normal and USA Standard) from data acquired during the autumn equinox period in 2009 along the DHO–Mikhnevo path and the corresponding N_e profile taken from GOST. As expected, the calculated profiles at all heights differ less than twofold, so in what follows the results obtained by using only the NO profiles from USA Standard (D-P model) are presented. Figure 8 shows that in the daytime of autumn months there is good agreement at h>65 km, but there is a difference at

the heights of the ionization by cosmic rays. It should be noted that at such low concentrations the difference is insignificant because the VLF reflection occurs above this area. In summer months of 2009, the situation is similar (Figure 9, *a*), but in winter months this difference is maximum at 70 km (Figure 9, *b*). Despite the relatively low average ionization rates in winter months (Figure 5), average N_e is larger than that in summer months. The analysis of the input experimental data for different seasons allows the conclusion that this is associated with the seasonal difference in T to which N_e is most sensitive. The nighttime values are almost identical in all seasons, and on the logarithmic scale they have a linear form (Figure 8, *b*).

The output parameters of the deterministic-probabilistic model of the ionospheric D-region are not average N_e but PDFs of N_e ($P(N_e)$). Advantages of the probabilistic approach can be seen by considering $P(N_e)$ at the points of the greatest difference between $\overline{N}_{e\,theor}$ and $\overline{N}_{e\,GOST}$ in the daytime of the autumn months in 2009, i.e., as follows from Figure 8, *a*, at the heights of 60 and 65 km. These probability density curves are shown in Figure 10. To construct the curves corresponding to GOST, all mid-latitude profiles of the selected season, solar activity, and time of day are combined. Also shown are the probability densities constructed from the experimental database on N_e [Nesterova, Ginzburg, 1985] (hereinafter Catalog), which contains the electronic profiles obtained with rockets, the method of partial reflections, etc. In Figure 8, at the selected heights $\overline{N}_{e\,GOST}$ exceeds $\overline{N}_{e\,theor}$, but Figure 10 shows that this shift is due to the heavy "tails" of $P(N_{eGOST})$, with much closer maximum values of the theoretical and GOST curves.

Maxima of the distributions constructed from Catalog at the two heights correspond to almost the same values of N_e as the maxima of the theoretical distributions.

In Figure 11 are curves representing summer months of 2009 at 75 and 80 km. Figure 9 shows that average $\overline{N}_{e\,theor}$ and $\overline{N}_{e\,GOST}$ at 75 km are in better agreement than those at 80 km; but in Figure 11 the most probable values of N_e at 80 km are obviously closer to each other than those at 75 km.
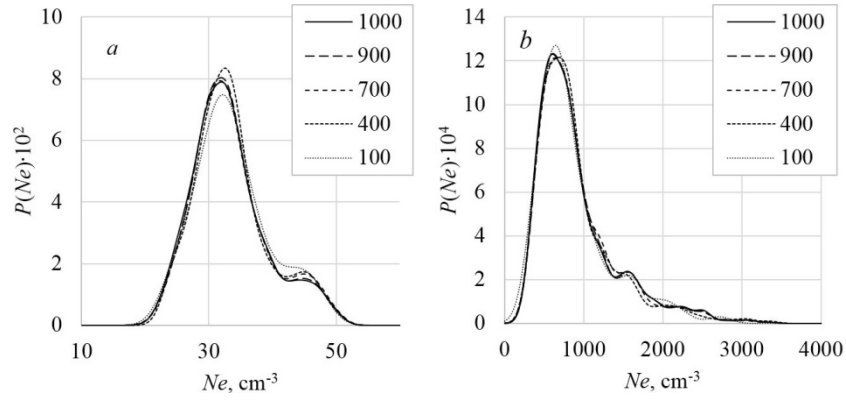
Figure 7. PDFs of N_e for h=60 km (*a*) and h=80 km (*b*) (daytime, autumn equinox period in 2009, midlatitudes)
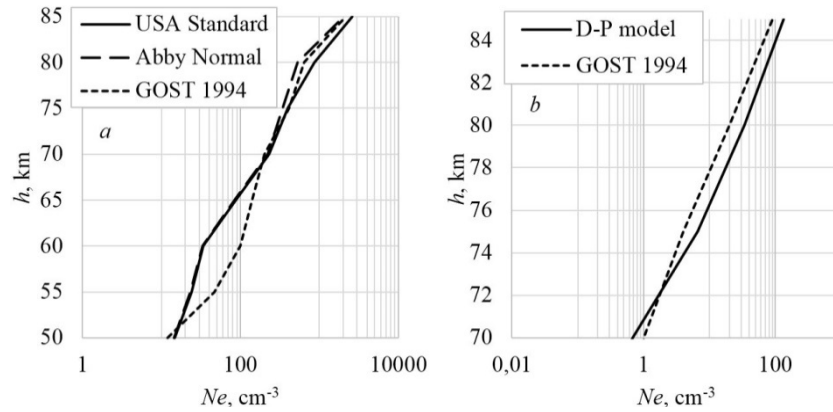

Figure 8. Average profiles of $\overline{N}_e$ for daytime (*a*) and nighttime (*b*) (autumn equinox period in 2009, midlatitudes)
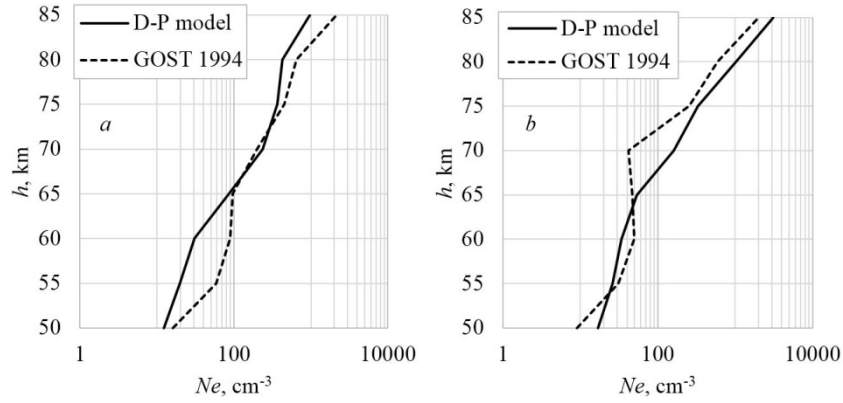

Figure 9. Average profiles of $\overline{N}_e$ for summer (*a*) and winter (*b*) months (daytime, 2009, midlatitudes)
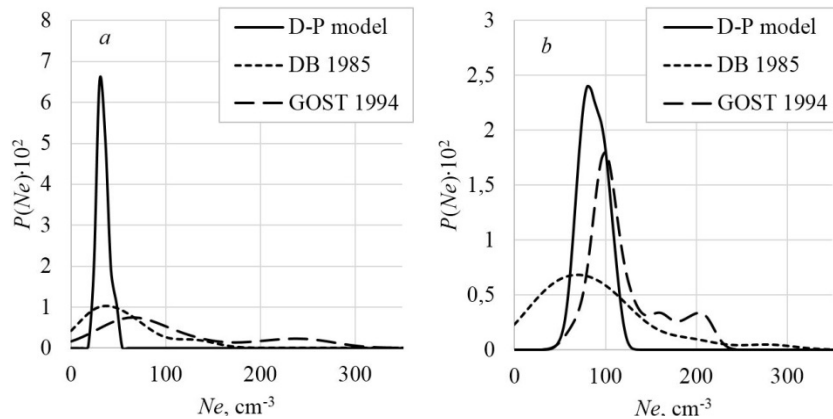

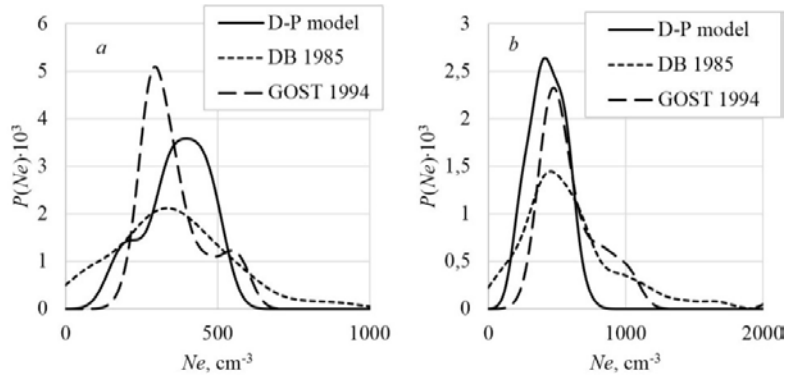*Figure 10.* PDFs of N_e for h=60 km (*a*) and h=65 km (*b*) (daytime, autumn equinox period in 2009, midlatitudes)

Figure 11. PDFs of N_e for *h*=75 km (*a*) and *h*=80 km (*b*) (daytime, summer months in 2009, midlatitudes)
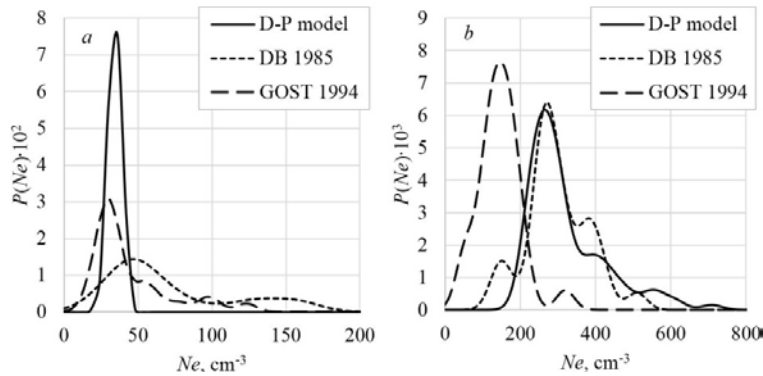

Figure 12. PDFs of N_e for *h*=60 km (*a*) and *h*=75 km (*b*) (daytime, winter months in 2009, midlatitudes)

Figure 12 demonstrates distributions as derived from data obtained during winter months in 2009. For the analysis, the heights of 60 and 75 km are selected at which the relative difference between $\bar{N}_{e\,theor}$ and $\bar{N}_{e\,GOST}$ is approximately the same, which is not the case for respective distributions. For example, the maximum values of the distributions at 60 km are very close, and at 70 km they obviously differ.

The analysis shows that the use of the median values do not allow correct conclusions about agreement between theoretical and experimental geophysical values.

In this work, the N_e probability density functions in midlatitudes have been calculated from data obtained in 2009, 2010, and 2012. In the daytime of summer months and equinox periods in years of low solar activity (2009 and 2010) at *h*>65 km, theoretical calculations are in good agreement with GOST data. At the lower part of the ionospheric D-region in these seasons, the model has the worst agreement with GOST and Catalog, but the orders of magnitude coincide even at these heights. In 2012, the situation is somewhat different: there appears a significant difference between GOST and Catalog, and the theoretical curves in different seasons are close to one or another database, or are somewhere between them.

CONCLUSION

Probabilistic modeling allows us to get away from a purely deterministic description of a medium, which is now widely used both in Russia and abroad. As shown above, the average value cannot give a true picture of the behavior of geophysical parameters because in most cases it does not coincide with the most probable value.

In conclusion, we emphasize again [Kozlov et al., 2014; Bekker et al., 2016] that any ionospheric model, including the deterministic-probabilistic model considered here, should be thoroughly verified using radiophysical experimental data. This stage of the study is of particular interest since the deterministic-probabilistic model, along with its obvious fundamental importance, has a distinctly applicable nature, and is primarily required to improve the accuracy of the forecast of VLF-LF radio wave propagation.

REFERENCES

Anderson G.P., Clough S.A., Kneizys F.X., Chetwynd J.H., Shettle E.P. Atmospheric Constituent Profiles (0–120 km). *Environmental Res. Papers*. 1986, no. 954, 46 p.

Bekker S.Z., Kozlov S.I., Lyakhov A.N. On some methods of increasing the accuracy of statistical models of the D-region of the ionosphere. *Trudy IV Vserossiiskoi nauchnoi konferentsii "Problemy voenno-prikladnoi geofiziki i kontrolya sostoyaniya prirodnoi sredy".* [Proc. the IV National Scientific Conference "Problems of the Military-Applied Geophysics and Environment Control"]. St. Petersburg, 2016, pp. 62–66. (In Russian).

Brunelli B.E. and Namgaladze A.A. *Fizika ionosfery* [Physics of the Ionosphere]. Moscow, Nauka Publ., 1988, 528 p. (In Russian).

Danilov A.D., Ledomskaya S.Y. Nitric oxide in the D-region. I. Experimental data of the [NO] distribution. *Geomagnetizm i aeronomiya* [Geomagnetism and Aeronomy], 1984, vol. 24, no. 4, pp. 614–619 (In Russian).

Egoshin A.A., Ermak V.M., Zetzer Yu.I., Kozlov S.I., Kudryavtsev V.P., Lyakhov A.N., Poklad Yu.V., Yakimenko E.N. Influence of meteorological and wave processes on the lower ionosphere during solar minimum conditions according to the data on midlatitude VLF–LF propagation. *Fizika Zemli* [Physics of the Solid Earth]. 2012, vol. 48, no. 3, pp. 275–286. (In Russian).

Heaps M.G. A parameterization of cosmic ray ionization. *Planet Space Sci*. 1978, vol. 26, pp. 513–517.

Kozlov S.I., Lyakhov A.N., Bekker S.Z. Key principles of constructing probabilistic statistical ionosphere models for the radiowave propagation problems. *Geomagnetizm i aeronomiya* [Geomagnetism and Aeronomy], 2014, vol. 54, no. 6, pp. 767–779. (In Russian).

Kotov Y.D. High-energy solar flare processes and their investigation onboard Russian satellite missions CORONAS. *Uspekhi fizicheskikh nauk* [Adv. in Physical Sciences], 2011, vol. 180, no. 6, pp. 647–661 (In Russian).

Koshelev V.V., Klimov N.N., Sutyrin N.A. *Aeronomiya mezosfery i nizhnei termosfery* [Aeronomy of the Mesosphere and Lower Thermosphere]. Moscow, Nauka Publ., 1983, 184 p. (In Russian).

Krivolutsky A.A., Repnev A.I. *Vozdeistvie kosmicheskikh faktorov na ozonosferu Zemli* [Impact of Space Factors on Earth's Ozonosphere]. Moscow, GEOS, 2009, 382 p. (In Russian).

Krivolutsky A.A., Cherepanova L.A., Vyushkova T.Yu., Repnev A.I. The three-dimensional numerical model CHARM-I: the incorporation of processes in the ionospheric D-region. *Geomagnetism and Aeronomy*. 2015, vol. 55, no. 4, pp. 468–487.

Krivolutsky A.A., Vyushkova T. Yu., Mironova I.A. Changes in chemical composition of the atmosphere in polar regions after solar proton flares (3D modeling). *Geomagnetism and Aeronomy*. 2017, vol. 57, no 2, pp. 173–194.

Moshchnye nadgorizontnye RLS dal'nego obnaruzheniya. Razrabotka. Ispytaniya. Funktsionirovanie [Powerful Over-Horizon Early Warning Radar. Development. Tests. Operation]. Ed. Boev S.F. Moscow, Radioengineering Publ., 2013, 168 p. (In Russian).

Nesterova I.I., Ginzburg E.I. *Katalog profilei elektronnoi kontsentratsii oblasti D ionosfery* [Catalog of the Electron Concentration Profiles of the Ionosphere D-region]. Novosibirsk, Inst. of Geology and Geochemistry Publ., 1985, 210 p. (In Russian).

Paulsen D.E., Huffman R.E., Larrabe J.C. Improved photoionization rates of $O_2(^1\Delta_g)$ in the D region. *Radio Sci*. 1971, vol. 7, no. 1, pp. 51–55.

Schumer E.A. *Improved modeling of midlatitude D-region ionospheric absorption of high frequency radio signals during solar x-ray flares*. Dissertation. Department of the Air Force Air University. Air Force institute of technology. 2009.

Shefov N.N., Semenov A.I., Khomich V.Yu. *Izluchenie verkhnei atmosfery – indikator ee struktury i dinamiki* [Upper Atmospheric Radiation As An Indicator of Its Structure and Dynamics]. Moscow, GEOS Publ., 2006, 741 p. (In Russian).

Thomas L., Bowman M.R. Model studies of the D-region negative-ion composition during day-time and night-time. *J. Atmos. Terr. Phys*. 1985, vol. 47, no. 6, pp. 547–556.

URL: http://saber.gats-inc.com/browse_data.php (accessed December 29, 2017).